Clin. Lab. 2026;72:XXX-XXX

ORIGINAL ARTICLE

Rapamycin and Cyclosporin A Alleviate Bone Marrow Adiposity in Murine Model of Aplastic Anemia

Qiuying Cao *, Liping Yang *, Mengyuan Liu, Pu Tang, Chunyan Liu, Zonghong Shao, Huaquan Wang

* *These authors contributed equally to this work and share first authorship*
Tianjin Key Laboratory of Bone Marrow Failure and Cancer Hematopoietic Cloning Prevention and Treatment, Tianjin Medical University General Hospital, Heping District, Tianjin, China

SUMMARY

Background: **Aplastic anemia (AA) is a bone marrow failure disease characterized by immune-mediated destruction of hematopoietic stem and progenitor cells. Bone marrow adiposity represents a typical pathological manifestation observed in AA.**
Methods: **The aim of this study was to establish a murine model of AA using immune-mediated methods and assess the impact of rapamycin (Rapa) and cyclosporin A (CsA) on bone marrow adiposity. The AA murine model was induced by 137Cs γ-ray irradiation and allogeneic lymphocyte infusion. Rapamycin and cyclosporine were administered intraperitoneally. Hematological parameters, bone marrow adiposity, and lipidomic profiles were evaluated. Gene and protein expression related to adipogenesis were analyzed.**
Results: **The Hematoxylin and Eosin (HE) and BODIPY staining results revealed an increase in adipocyte area and a decrease in hematopoietic area in AA murine. Relative expression levels of PPAR-γ, LPL, and Ap2 mRNA were significantly elevated in bone marrow mononuclear cells (BMMNCs) from the AA group. Lipidomics analysis indicated notable differences between the AA group and the normal group regarding lipid metabolism, particularly concerning glycerolphospholipids. Following treatment with Rapa and CsA, not only did the hematological profile of AA murine recover, but there was also a reduction in bone marrow adiposity in HE and BODIPY staining and a decrease in the gene and protein expression of PPAR-γ, LPL, and Ap2. The lipidomic analysis revealed a reduction in the lipid metabolism of AA murine following Rapa and CsA treatment in AA murine, particularly acylcarnitin (ACar), phosphatidylserine (PS) and phosphatidylethanolamine (PE). The enrichment results of the KEGG pathway analysis demonstrated a statistically significant role of C42H82N010P in glycerophospholipid metabolism.**
Conclusions: **Our study used lipidomics for the first time to investigate lipid metabolism in AA murine, revealing that Rapa and CsA primarily downregulate glycerophospholipid metabolism as a means to alleviate bone marrow adiposity in AA murine.**
(Clin. Lab. 2026;72:xx-xx. DOI: 10.7754/Clin.Lab.2025.250207)

Correspondence:
Zonghong Shao
Tianjin Medical University General Hospital
154 Anshan Street, Heping District
Tianjin
China
Phone: + 86 13802036467
Fax: + 86 02260817092
Email: shaozonghong@tmu.edu.cn

Huaquan Wang
Tianjin Medical University General Hospital
154 Anshan Street, Heping District
Tianjin
China
Phone: + 86 18222039795
Fax: + 86 02260817073
Email: wanghuaquan@tmu.edu.cn

Manuscript accepted June 4, 2025

KEYWORDS

aplastic anemia, bone marrow adiposity, rapamycin, cyclosporin A, glycerophospholipid

INTRODUCTION

Aplastic anemia (AA) is a disorder characterized by bone marrow failure, presenting with pancytopenia and reduced bone marrow hematopoietic stem and progenitor cells (HSPCs). In most cases, this condition arises from an immune attack by autoreactive T cells against HSPCs. This leads to the replacement of normal hematopoietic tissue with bone marrow adipose tissue [1,2]. The bone marrow (BM) is a heterogeneous tissue located in the medullary canal of long bones such as the femur, tibia, and humerus, as well as in flat bones like the iliac crest and sternum. It comprises various cell types, including hematopoietic and stromal cells. Hematopoietic cells encompass myeloid cells, erythroid cells, and lymphocytes, while stromal cells include adipocytes, osteoblasts, chondrocytes, and bone marrow stromal cells.

Bone marrow adipocytes (BMAds) constitute the largest cellular population within the bone marrow cavity and represent the third most significant adipose reservoir in the human body [3]. BMAds play a crucial role as a constituent of the bone marrow microenvironment, exerting their influence on hematopoiesis through direct interaction with hematopoietic cells and via secretion of adipokines by adipocytes [4]. In cases of AA, the differentiation of bone marrow mesenchymal stem cells (BMMSCs) becomes imbalanced, with an increase in adipocyte differentiation and a decrease in osteoblast differentiation [5].

For many years, the focus in the clinical development of the nontransplant therapies for AA has been on intensifying immunosuppressive therapy (IST), usually as antithymocyte globulin (ATG) and cyclosporin A (CsA), which have dramatically changed the course of this illness, with the 10-year survival rate of patients now at about 70% [6]. However, about 30% of patients still have poor treatment response, and about 10% of responders relapse, while 16% of patients have treatment-related deaths due to drug-related side effects [7]. Therefore, a novel immunosuppressive regimen to circumvent these problems is needed. The anti-fungal macrolide rapamycin (Rapa) is an mTOR kinase inhibitor isolated from the soil bacterium streptomyces hygroscopicus. Rapamycin produces inhibiting effects by binding to the immunophilin FK506 binding protein (FKBP12) to form a complex, which then binds directly to mTOR, inhibiting mTOR and the mTOR-mediated signaling network. Subsequently, rapamycin was shown to have potent immunosuppressive and antiproliferative effects. As an immunosuppressant drug, it is used extensively following kidney, liver, and heart transplants to prevent acute graft rejection [8]. In recent years, Feng et al. reported that rapamycin effectively treated immune-mediated murine BM failure as compared to the standard-dose CsA, which showed a high efficacy in suppressing Th1 immune responses, eradicating pathogenic CD8+ T cells [9]. However, limited research has been conducted on this aspect at present.

In recent years, the field of lipidomics has garnered increasing recognition as a novel and prospective biomarker discovery platform. It has been instrumental in the early detection, progression monitoring, and therapeutic management of various malignancies and additional pathologies. Notably, distinct lipidomic profiles have been detected across hematological diseases, albeit predominantly within hematological malignancies [10-12]. Nevertheless, there remains a paucity of research focusing on the lipidome in AA. In this study, in addition to observing the level of bone marrow adiposity in AA murine via multifaceted approaches, we elucidated the impacts of rapamycin and CsA on modulating bone marrow adiposity in AA murine. Additionally, this study represented the first to delve into the alterations of bone marrow lipid metabolism in AA murine, thereby offering a novel research avenue for the advancement of AA immunotherapeutic strategies.

MATERIALS AND METHODS

Establishment of a murine model for AA

Lymphocyte suspensions were prepared from the thymus and spleen of donor mice. C57BL/6J female murine (Beijing Vitalstar Biotechnology Co., Ltd., China) were selected as donor murine. The donor murine were euthanized and soaked in trays containing 75% ethanol. Under aseptic conditions, the spleens and thymus were dissected and were placed in 6-cm sterile Petri dishes containing RPMI 1640 complete medium, which included 10% fetal bovine serum and 1% penicillin/streptomycin. The samples were transferred to the 70-μm cell filters using sterile forceps. Single-cell suspensions of thymus and spleen lymphocytes from donor murine were obtained by gently grinding the tissues. Finally, sterile PBS buffer was added to resuspend the single nucleated cells. Cell counts were performed under an inverted optical microscope. The prepared cell suspension was stored in the refrigerator at 4°C for future use. Recipient murine were irradiated with 4.5Gy 137Cs γ-rays. B6D2F1 murine (Beijing Vitalstar Biotechnology Co., Ltd., China) were selected as the recipient murine and were irradiated with a total dose of 4.5Gy 137Cs γ-rays at a dose rate of 90 cGy/minute in the Rapa, CsA, and AA groups at day 0, while the normal group was given pseudo-irradiation (lead-brick shielding from γ-rays). B6D2F1 female murine received lymphocyte infusion: B6D2F1 female murine in the Rapa, CsA, and AA groups were injected intraperitoneally with a prepared lymphocyte mixture of donor murine of 8×10^6 lymphocytes per murine, and an equal volume of saline was given to B6D2F1 female murine in the

normal group within 4 - 6 hours after irradiation. The day of intraperitoneal injection was recorded as day 0, and the murine model of immune-mediated acquired AA was prepared at day 12.
This study was approved by the Animal Ethics Committee of the General Hospital of Tianjin Medical University.

***In vivo* injection of rapamycin and CsA into murine**
One hour after the completion of 4.5Gy 137Cs γ-ray whole body irradiation and intraperitoneal injection of donor lymphocytes in the Rapa, CsA, and AA groups, each murine in the rapamycin group was given intraperitoneal injections of rapamycin (TargetMol Chemicals Inc. Boston, MA, USA) at the dose of 2 mg/kg/day every 24 hours, day 0 - 12. Each murine in the CsA group was given intraperitoneal injections of CsA (TargetMol Chemicals Inc. Boston, MA, USA) at the dose of 25 mg/kg/day every 24 hours, day 0 - 9. The same volume of saline was injected intraperitoneally into each murine in the AA group.
Due to technical challenges and budgetary constraints encountered during the experiment, 12 mice were ultimately included for final analysis. Consequently, the final cohort sizes were standardized at n = 3 per group across all experimental conditions: Normal controls, AA model, CsA treatment, and Rapa treatment groups.

Peripheral blood specimen collection and blood cell count level testing
On days 4, 8, and 12 of the establishment of the aplastic anemia model in the Rapa, CsA, AA, and normal groups of murine, blood was collected from the retro-orbital venous plexus using capillary blood collection tubes of 0.5 x 100 mm size, 80 - 100 μL per murine, and the blood specimens were placed in EDTA anticoagulated 1.5 mL EP tubes and put into a 4°C cold refrigerator for detection by automatic blood cell analyzer.

Hematoxylin and Eosin (HE) staining of femoral bone marrow
On day 13, left femur specimens from murine were fixed in 4% paraformaldehyde solution at low temperature for 24 hours, followed by decalcification in EDTA solution. The specimens underwent ethanol dehydration, were rendered transparent in xylene I and xylene II, and were subsequently embedded in paraffin wax. After solidification, the wax blocks were sectioned into 3 - 5 μm slices, placed on slides, and baked at 45°C for approximately 25 minutes. Deparaffinization was carried out using xylene, followed by application of gum and coverslips for sealing. The prepared slides were then observed under a light microscope for examination.

Assessment of bone marrow adiposity using BODIPY
Initially, the left femur of the murine was surgically extracted under sterile conditions and immersed in a 1.5 mL EP tube filled with a 10% formalin solution, which was then stored at 4°C for 24 hours to facilitate tissue fixation. Following fixation, the tissue underwent dehydration in a 20% sucrose solution. Subsequently, the dehydrated tissue was encased in optimal cutting temperature compound, snap-frozen, and embedded for sectioning using a Thermo HM525NX microtome. Slices of 5 - 10 μm thickness were affixed to slides and stored at -20°C. Before staining, the stored tissues were gently rewarmed at room temperature for 15 minutes. The cell membrane was then permeabilized using a 0.1% cell membrane-breaking solution for 15 minutes, followed by immersion in TBS with Tween-20. A 1:500 dilution of BODIPY staining solution (Thermofisher, USA) was applied (50 μL per section) and left to incubate at 37°C for 60 minutes. Post-incubation, sections were rinsed with TBST thrice, each time for 5 minutes. A working solution of 4',6- diamidino-2-phenylindole (1:500) was administered (50 μL per section) for nuclear staining, followed by a 5-minute light-protected rinse with TBS containing Tween-20. Finally, sections were hermetically sealed using a fluorescent sealer (Suthern biotech, USA) and subsequently subjected to microscopic examination.

Real-time quantitative transcriptase-polymerase chain reaction (qRT-PCR)
1 x 10^6 murine bone marrow mononuclear cells (BMMNCs) were collected. Total RNA was extracted using TRIzol (Takara Bio USA Inc.), and cDNA was generated using a reverse transcriptase kit (Takara Bio USA Inc.). The gene expressions were quantified by Q-PCR (SYBR® Premix Ex Taq II, Takara Bio, China). The primer sequences were as follows:
PPAR forward
5'- CCAAGAATACCAAAGTGCGATC -3',
reverse
5'- TCACAAGCATGAACTCCATAGT -3';
LPL forward
5'- GGGAGTTTGGCTCCAGAGTTT -3',
reverse
5'- TGTGTCTTCAGGGGTCCTTAG -3';
Ap2 forward
5'- TCACCGCAGACGACAGGAAGG -3',
reverse
5'- TAACACATTCCACCAGCTTGTCACC -3';
GAPDH forward
5'- TGAAGCAGGCATCTGAGGG -3',
reverse
5'- CGAAGGTGGAAGAGTGGGAG -3'.
To generate the relative quantification (RQ) of the gene expression, the $2^{-\Delta\Delta Ct}$ method was used.

Western blotting
The total proteins of murine BMMNCs were extracted by lysis buffer (Biotech, Beijing, China). Protein concentration was determined using the Pierce BCA Protein Assay Kit (Thermo Scientific, USA). Samples were separated by 4 - 20% SDS-PAGE gels and then trans-

ferred to PVDF membranes (PE, USA) by Trans-Blot Cell system (Bio-Rad, USA) using standard Western blotting procedures. The membranes were probed with rabbit anti-murine PPAR-γ, LPL, Ap2, and GDPDH monoclonal antibody (Cell Signaling Technology, USA) at 1:1,000 and incubated overnight at 4°C. The sheep anti-rabbit *β*-actin antibody (Santa Cruz Biotechnology Inc., sc-47778, USA) at 1:5,000 was used as loading control. The goat anti-rabbit IgG HRP-conjugated secondary antibody (Santa Cruz Biotechnology Inc., sc-2054, USA) was incubated for 1 hour at room temperature. After washing, an electrochemiluminescence (ECL) reagent (Thermo Scientific, number 321 06, USA) was used for chemiluminescence.

Lipidomics of BMMNCs

Lipid extraction

Methanol (0.75 mL) was added to a 1 x 10^7 BMMCs, which was placed into a glass tube with a Teflon lined cap, and the tube was vortexed. Next, 2.5 mL of MTBE was added and the mixture was incubated for 1 hour at room temperature in a shaker. Phase separation was induced by adding 0.625 mL of MS-grade water. Upon 10 minutes of incubation at room temperature, the sample was centrifuged at 1,000 g for 10 minutes. The upper (organic) phase was collected, and the lower phase was re-extracted with 1 mL of the solvent mixture (MTBE/methanol/water (10:3:2.5, v/v/v)). Combined organic phases were dried and dissolved in 100 µL of isopropanol for storage, then analyzed by LC-MS/MS.

UHPLC-MS/MS analysis

UHPLC-MS/MS analyses were performed using a Vanquish UHPLC system (Thermo Fisher, Germany) coupled with an Orbitrap Q ExactiveTM HF mass spectrometer (Thermo Fisher, Germany) in Novogene Co., Ltd. (Beijing, China). Samples were injected into a Thermo Accucore C30 column (150 x 2.1 mm, 2.6 µm) using a 20-minute linear gradient at a flow rate of 0.35 mL/minute. The column temperature was set at 40°C. Mobile phase buffer A was acetonitrile/water (6/4) with 10 mM ammonium acetate and 0.1% formic acid, whereas buffer B was acetonitrile/isopropanol (1/9) with 10 mM ammonium acetate and 0.1% formic acid. The solvent gradient was set as follows: 30% B, initial; 30% B, 2 minutes; 43% B, 5 minutes; 55% B, 5.1 minutes; 70% B, 11 minutes; 99% B, 16 minutes; 30% B, 18.1 minutes. Q ExactiveTM HF mass spectrometer was operated in positive [negative] polarity mode with sheath gas: 40 psi, sweep gas: 0 L/minute, auxiliary gas rate: 10 L/minute [7 L/minute], spray voltage: 3.5 kV, capillary temperature: 320°C, heater temperature: 350°C, S-Lens RF level: 50, scan range: 114 - 1,700 m/z, automatic gain control target: 3e6, normalized collision energy: 22 eV; 24 eV; 28 eV [22 eV; 24 eV; 28 eV], injection time: 100 ms, isolation window: 1 m/z, automatic gain control target (MS2): 2e5, dynamic exclusion: 6 seconds.

Data search

The raw data files generated by UHPLC-MS/MS were processed using the Compound Discoverer 3.01 (CD3.1, Thermo Fisher) to perform peak alignment, peak picking, and quantitation for each metabolite. The main parameters were set as follows: retention time tolerance, 0.2 minutes; actual mass tolerance, 5 ppm; signal intensity tolerance, 30%; signal/noise ratio, 3; and minimum intensity, 100,000. After that, peak intensities were normalized to the total spectral intensity. The normalized data was used to predict the molecular formula based on additive ions, molecular ion peaks and fragment ions. And then peaks were matched with the Lipidmaps and Lipidblast database to obtain the accurate qualitative and relative quantitative results. Statistical analyses were performed using the statistical software R (R version R-3.4.3), Python (Python 2.7.6 version), and CentOS (CentOS release 6.6). When data were non-normally distributed, normal transformations were attempted by using area normalization method.

Data analysis

Principal components analysis (PCA) and partial least squares discriminant analysis (PLS-DA) were performed at metaX (a flexible and comprehensive software for processing metabolomics data). We applied univariate analysis (*t*-test) to calculate the statistical significance (p-value). The metabolites with VIP > 1 and p-value < 0.05 and fold change ≥ _2 or FC ≤ _0.5 were considered to be differential metabolites. Volcano plots were used to filter metabolites of interest, which were based on Log2 (FC) and -log10 (p-value) of metabolites.

For clustering heat maps, the data were normalized using z-scores of the intensity areas of differential metabolites and were plotted by Pheatmap package in R language. The correlation between differential metabolites were analyzed by cor () in R language (method = Pearson). Statistically significant of correlation between differential metabolites were calculated by cor.mtest () in R language. p-value < 0.05 was considered as statistically significant, and correlation plots were plotted by corrplot package in R language.

Statistical analysis

All data were analyzed by GraphPad Prism 8.0 software (GraphPad Software, Inc., San Diego, CA) and presented as mean ± standard deviation. Two group comparisons were performed using *t*-test, and multiple group comparisons were performed using one-way analysis of variance (ANOVA). Correlation analyses were performed by Spearman rank correlation. p-value of < 0.05 was considered statistically significant.

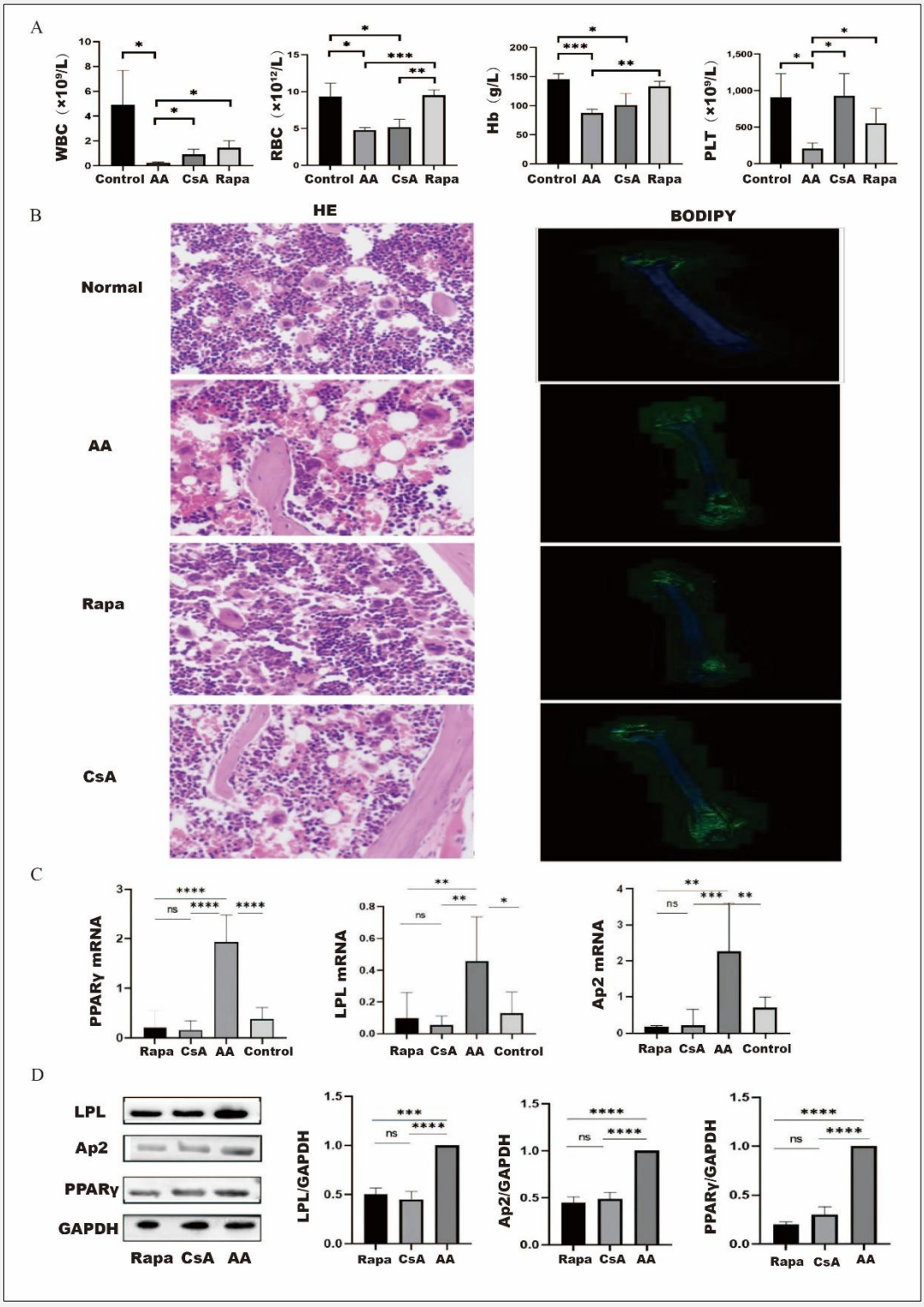

Figure 1. A The blood cell count levels in peripheral blood of murine on day 12. B HE staining (left panels) and BODIPY immunohistochemistry technology (right panels) detected the levels of bone marrow adipocytes in each group on day 13. C RT-qPCR detected the relative mRNA expression levels of PPAR-γ, LPL, and Ap2 in BMMNCs in each group. D Western blot detected the protein expression levels of PPAR-γ, LPL, and Ap2 in BMMNCs of each group.
*** $p < 0.05$, ** $p < 0.01$, *** $p < 0.001$.**

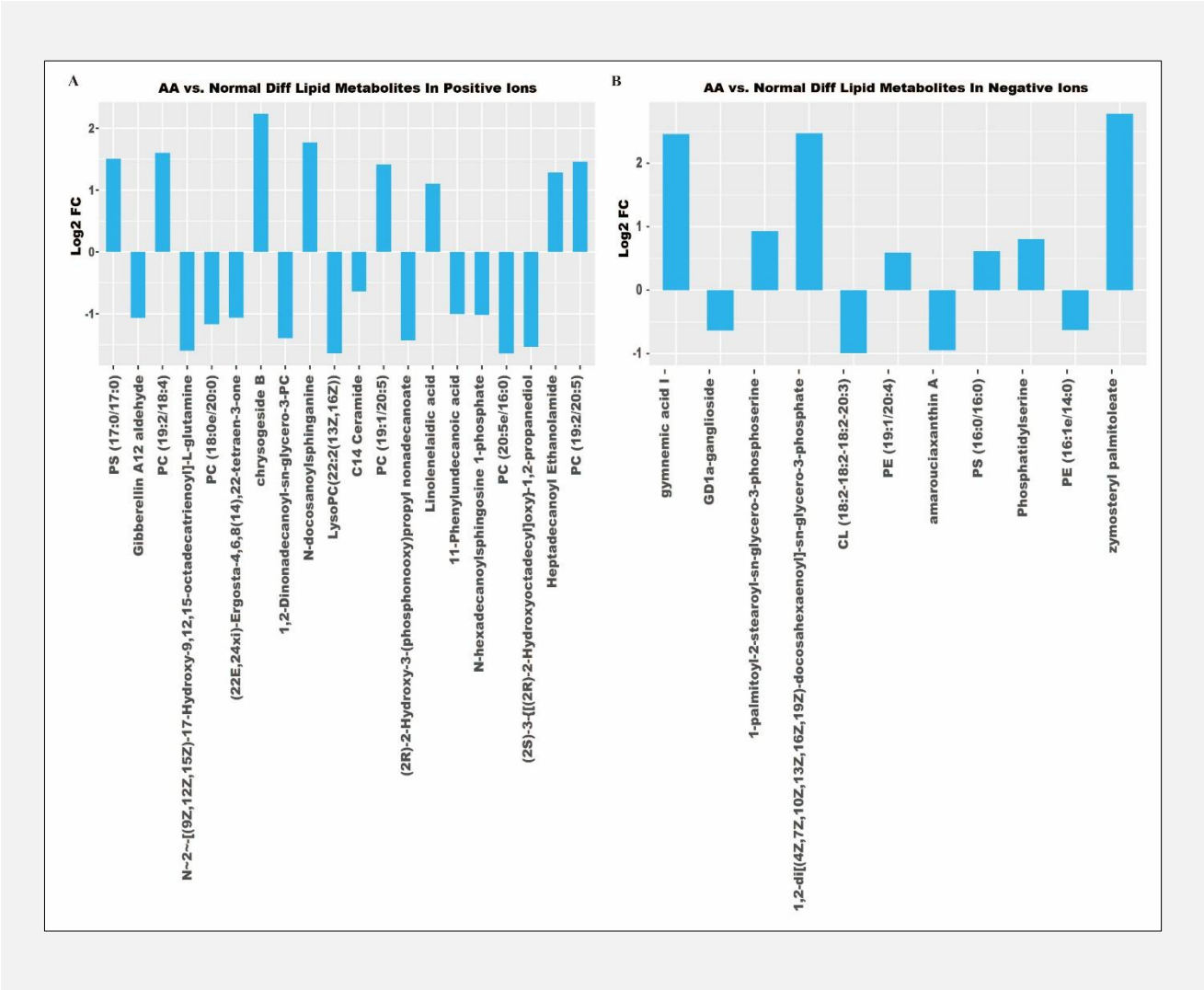

Figure 2. Lipidomic comparison of distinct lipid compounds between AA murine and control group in both positive A) and negative B) ions.

RESULTS

The level of bone marrow adiposity in AA murine was found to be higher compared to the normal control by multiple techniques

The AA murine model was successfully established as the pancytopenia was achieved in our study. By day 12, the counts of WBC, RBC, Hb, and PLT in the peripheral blood of the AA group were lower compared with the normal group (Figure 1A).

HE staining revealed that the normal group displayed vigorous nucleated cell proliferation, constituting approximately 69% of the hematopoietic area, with a lower adipocyte area of about 31%. Megakaryocyte count was notably higher at approximately 15 per high-power field (HP). Conversely, the AA group exhibited a significant reduction in nucleated cell proliferation, with a hematopoietic area of roughly 23%, a higher adipocyte area of approximately 77%, and a notably lower megakaryocyte count of about 5/HP (Figure 1B). BODIPY immunohistochemistry results indicated that AA murine had significantly more adipocytes than the normal group (Figure 1B). The relative expression levels of PPAR-γ, LPL, and Ap2 mRNA in BMMNCs from the AA group were significantly higher compared to the normal group (Figure 1C and D).

Combined with lipidomics analysis, we observed significant disparities in lipid metabolism between the AA group and the control group, particularly in glycerophospholipids such as phosphatidylcholine (PC) and phosphatidylserine (PS). PC represented by PC (19:2/18:4), PC (19:1/20:5), PC (19:2/20:5), etc., PS represented by PS (17:0/17:0), 1-palmitoyl-2-stearoyl-sn-glycero-3-phosphoserine, and PS (16:0/16:0) were elevated. The levels of compounds such as PC (18:0e/20:0), LysoPC (22:2 (13Z,16Z)), PC (20:5e/16:0), etc. were

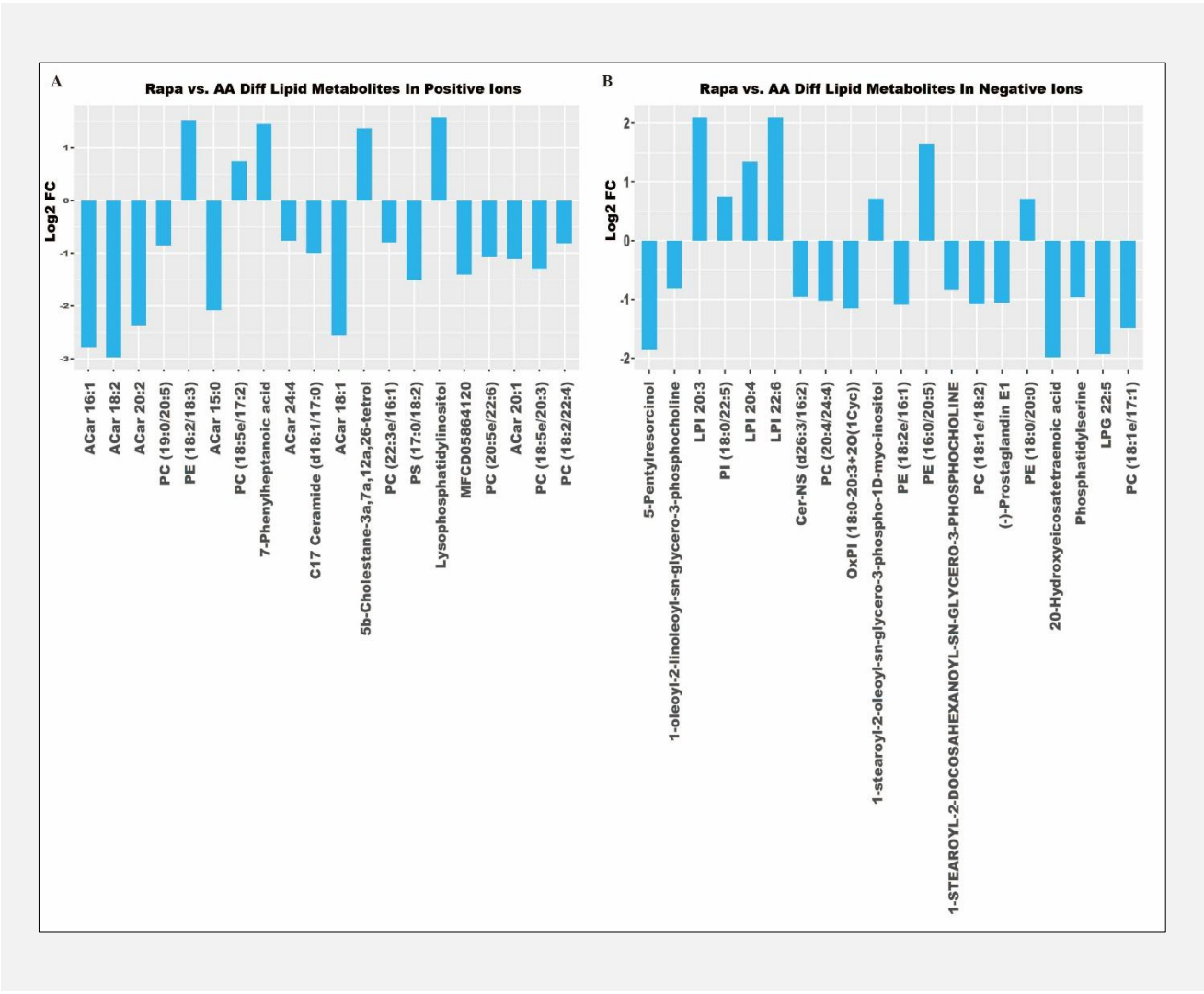

Figure 3. Lipidomic comparison of distinct lipid compounds between Rapa group and AA murine in both positive A) and negative B) ions.

reduced (Figure 2).

In summary, we confirmed through multifaceted approaches that the level of bone marrow adiposity in AA murine is higher compared to the normal group. Additionally, there is a replacement of normal hematopoietic tissue with adipocytes, and an increase in lipid synthesis metabolism primarily represented by PS and PC in AA murine.

Rapamycin and cyclosporin A alleviate bone marrow adiposity in AA murine

By day 12, the Rapa group showed an improvement in peripheral blood leukocyte and hemoglobin levels compared to the AA group. Nevertheless, there was no statistically significant difference observed in the platelet levels in the AA group (Figure 1A). In the Rapa group, there was robust nucleated cell proliferation, constituting around 60% of the hematopoietic area, with a lower adipocyte area of about 40%. Megakaryocyte presence was estimated at approximately 14/HP. The BODIPY immunohistochemical technique enables enhanced detection of Rapa, leading to a significant improvement in bone marrow adiposity in AA murine (Figure 1B). Following intervention with Rapamycin, both the expression of PPAR-γ, LPL, and Ap2 mRNA and proteins in murine BMMNCs were notably downregulated (Figure 1D and E).

The lipidomic analysis revealed a reduction in the lipid metabolism of AA murine following Rapa treatment, particularly Acylcarnitin (ACar) represented by ACar 16:1, ACar 18:2, ACar 20:2, ACar 18:1, ACar 20:1, etc., PC represented by PC (19:0/20:5), PC (18:1e/17:1), 1-oleoyl-2-Linoleoyl-SN-3-phosphocholine, PC (20:4/24:4), PC (18:e/18:2), etc. were reduced (Figure 3).

The CsA group displayed a generally normal degree of

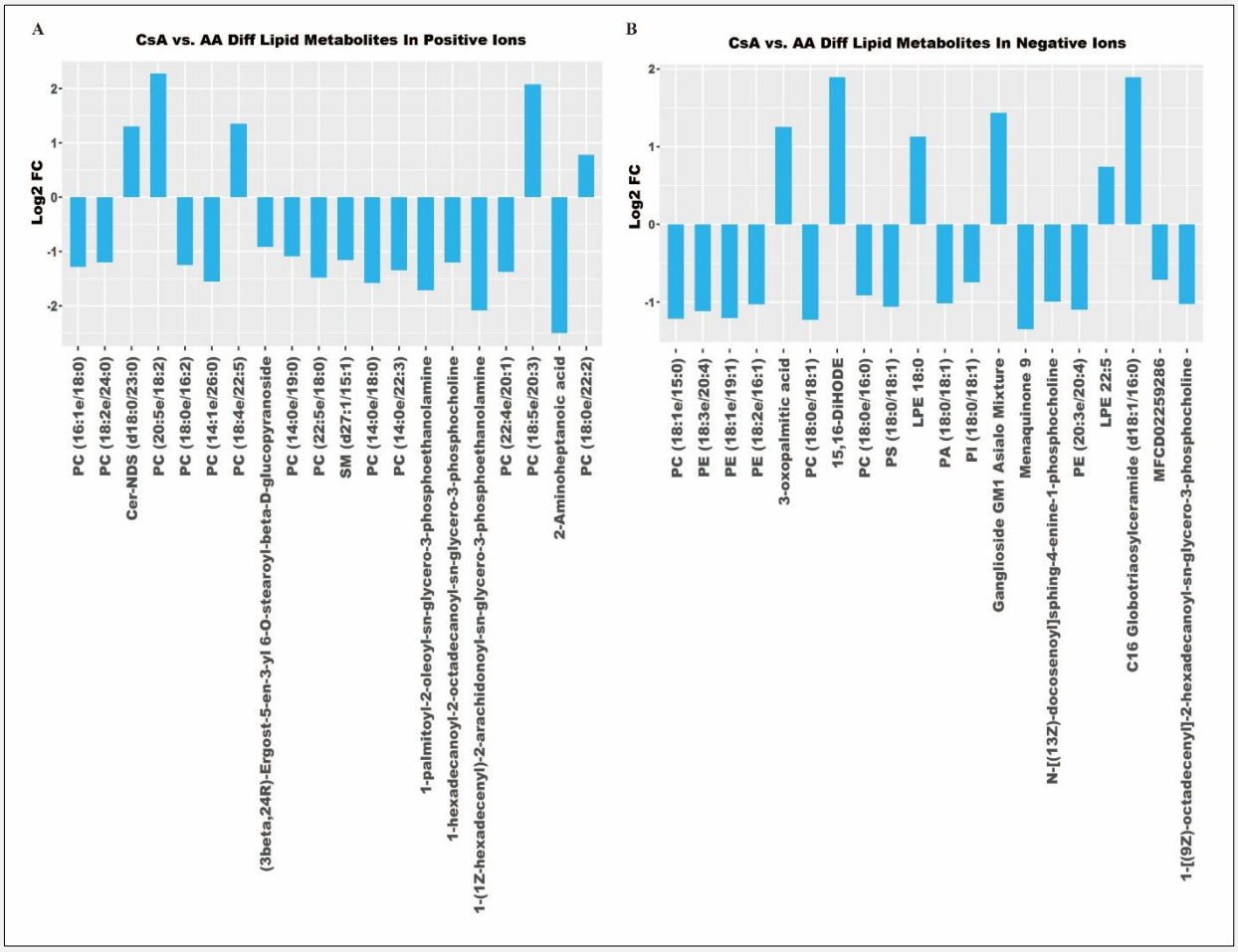

Figure 4. Lipidomic comparison of distinct lipid compounds between CsA group and AA murine in both positive A) and negative B) ions.

nucleated cell proliferation, with a hematopoietic area of approximately 40% and an adipocyte area of about 60%. The number of megakaryocytes was relatively lower, estimated at approximately 10/HP. Similarly, the BODIPY immunohistochemical technique enables the enhanced detection of CsA, leading to a significant improvement in bone marrow adiposity in AA murine (Figure 1B). Following intervention with CsA, both the expression of PPAR-γ, LPL, and Ap2 mRNA and proteins in murine BMMNCs were notably downregulated (Figure 1D and E).

The lipidomics results revealed a significant downregulation of numerous PC compounds following CsA treatment in AA murine, represented by 1-hexadecanoyl-2-octadecanoyl-sn-glycero-3-phosphocholine, 1-(1Z-hexadecenyl)-2-arachidonoyl-sn-glycero-3-phosphoethanolamine, PC (18:0e/16:2), PC (16:1e/18:0), and accompanied by a decrease in the levels of PE (18:3e/20:4), PE (20:3e/20:4) certain phosphatidylethanolamine (PE) compounds as well (Figure 4).

Rapamycin and CsA may alleviate bone marrow adiposity in AA murine through glycerophospholipid metabolic pathway

The levels of PC (18:3e/20:0), PC (18:3e/22:1), 1-(1Z-hexadecenyl)-2-arachidonoyl-sn-glycero-3-phosphoethanolamine, ACar 14:0, PC (20:3e/16:0), PA (16:0/18:1), 1-hexadecyl-2-hexadecanoyl-sn-glycero-3-phosphocholine, PE (18:0e/15:0), PC (18:1e/17:1), PC (18:1e/15:0), PC (18:1e/18:2), PS (19:0/18:2), Dihomo-I^3-Linolenoyl PAFC-16, PE (18:2e/16:1), and PC (18:1e/22:3) exhibited a decrease following treatment with Rapa and CsA, although no statistically significant increase was observed in the AA group.

By comparing the differences in lipid compounds between groups, we were surprised to discover that PS (C42 H82 N 010 P), which exhibited elevated levels in AA murine and decreased after treatment with Rapa and CsA, appears to be a pivotal target for regulating bone marrow lipid metabolism in AA murine. The enrichment results of the KEGG pathway analysis demonstrated a statistically significant role of PS (C42H82N 010P) in glycerophospholipid metabolism.

DISCUSSION

AA is characterized by bone marrow hematopoietic failure, leading to panocytopenia. Notably, the replacement of bone marrow hematopoietic tissue with adipocytes represents a significant pathological feature in patients with AA. However, there has been limited attention given to bone marrow adiposity in AA patients, and its underlying mechanism and potential significance remain unclear. In this study, we primarily investigated the therapeutic effects of Rapa and CsA on bone marrow adiposity and lipid metabolic dysregulation in AA murine models.

Our data demonstrate that Rapa and CsA significantly downregulated adipogenesis-associated factors (PPAR-γ, LPL, Ap2) in AA murine models. PPAR-γ, a transcription factor activated by ligands, is expressed in both preadipocytes and BMMSCs, exerting a pivotal role in regulating adipose differentiation. By inhibiting T cell activation, the PPAR-γ antagonist GW9662 effectively ameliorated panhemopenia and bone marrow failure in AA murine [13]. Research has indicated that PPAR-γ assumes an inhibitory function in hematopoiesis regulation, with its expression level demonstrating a negative correlation with the proportion of hematopoietic cells in the bone marrow [14,15]. Inhibiting PPAR-γ has shown to expedite hematopoietic recovery in murine following bone marrow failure. Activation of mTOR signaling leads to an increase in PPAR-γ levels, thereby promoting enhanced the differentiation of preadipocytes and facilitated adipogenesis in cells, indicating its potential role in inducing lipid accumulation [16, 17]. Conversely, inhibition of mTOR can suppress PPAR-γ activity, thereby reducing fat formation and differentiation. Rapamycin protects against high-fat diet-induced obesity in C57BL/6J murine. Previous studies have demonstrated that murine treated with Rapa, compared with the high-fat diet (HFD) control murine, exhibited a reduction in body weight and epididymal fat pads/body weight, along with reduced daily food efficiency, and lower serum leptin and insulin levels. However, Rapa-treated murine were hyperphagic, demonstrating an increase in food intake. Dissection of Rapa-treated murine revealed a marked reduction in fatty liver scores, average fat cell size, and percentage of large adipocytes of retroperitoneal and epididymal white adipose tissue, compared to the HFD control murine. These results suggest that Rapa prevented the effect of the high-fat diet on the rate of accretion in body weight via reducing lipid accumulation, despite greater food intake [18]. Rapa promotes triacylglycerol lipolysis and release of free fatty acids in 3T3-L1 adipocytes. Additionally, it was observed that treatment of 3T3-L1 adipocytes with Rapa resulted in a significant 50% reduction in insulin-stimulated triacylglycerol (TAG) accumulation. Further evidence suggests that Rapa synergistically inhibits mTORC1 signaling along with the β-adrenergic-CAMP/PKA pathway to enhance hormone-sensitive lipase (HSL) phosphorylation and facilitate hormone-induced lipolysis [19]. Enhanced by previous research on the therapeutic application of Rapa in AA, it becomes evident that rapamycin effectively modulates bone marrow functionality, encompassing both immune response and lipid metabolism through the mTOR signaling pathway, thereby offering a potential treatment for AA.

The nuclear factor of activated T cells (NFAT) is a family of transcription factors found in 3T3-L1 adipocytes and MSCs, playing a crucial role in adipocyte differentiation. CsA effectively hinders the nuclear translocation of NFAT, thereby impeding the process of adipocyte differentiation [20]. CsA treatment remarkably attenuates food intake and body weight gain in the obese murine. RT-PCR analysis of genes involved in adipocyte differentiation and lipid metabolism in white adipose tissue reveal that CsA application reduces expression of PPAR-γ, Fas, and Scd 1. The productions of proinflammatory cytokines (IL-1β, IL-2, IL-12, and TNFα) and JNK activity were remarkably reduced in the CsA-treated obese animals. These results suggest that CsA treatment might play beneficial effects against obesity [21]. The immunosuppressive agents Rapa and CsA increase lipolysis, inhibit lipid storage, and alter expression of genes involved in lipid metabolism in human adipose tissue [22].

Lipidomics revealed that Rapa and CsA predominantly downregulated glycerophospholipids (PS, PC, PE) in AA murine, implicating glycerophospholipid metabolism as a central pathway in marrow lipidosis. Additionally, this pathway may also serve as an important signaling mechanism for Rapa and CsA in improving bone marrow lipification in AA murine. Based on head group structures, glycerophospholipids are subdivided into classes, including PC, PE, PS, phosphatidic acid (PA), phosphatidylinositol (PI), phosphatidylglycerol (PG), and cardiolipin (CL). PC is the most abundant phospholipid in mammalian cells, and all mammalian cells synthesize PC via the cytidine diphosphate (CDP)-choline pathway. PE is the second most abundant phospholipid in the mammalian cell membrane. In mammalian cells, PE is produced through the CDP-ethanolamine and PS decarboxylation pathways. PS is a quantitatively minor component of mammalian cell membranes, namely 2% - 10% of total phospholipids. In plasma membranes, the majority of PS molecules resides on the inner leaflet of the bilayer. In mammalian cells, PSS catalyzes the exchange of l-serine with the

choline moiety of PC or ethanolamine moiety of PE [23,24]. In addition to their structural roles in membranes, phospholipids play important roles in various cellular processes, such as membrane trafficking, membrane protein localization and regulation, autophagy, cellular signaling, cell proliferation and differentiation, cell migration, and apoptosis. Impaired glycerophospholipid metabolism leads to diverse disorders, including dyslipidemia, atherosclerosis, liver diseases, respiratory diseases, autoimmune diseases, neurological diseases, cardiac and skeletal myopathies, and cancers [25]. In previous study, serum lipid profiles were explored in AA patients before and after CsA treatment. AA patients had decreased arachidonic acid pathway metabolites and retinol metabolism-related metabolites compared with the healthy ones. After 6 months of CsA treatment, serum arachidonic acid, PGE2, PGJ2, 15(S)-HETE, leukotriene B4, and protectin D1 decreased significantly. Patients who had response to CsA had higher levels of baseline protectin D1, leukotriene B4, 15(S)-HETE, and all-trans-retinal than those who had no response [26].

Bone marrow adipose tissue (BMAT) encompasses a heterogeneous population of mature adipocytes and preadipocytes, with distinct morphologies, lipid content, gene expression, and function. Preadipocytes are characterized by the expression of early adipogenic genes (PPAR-γ and CEBPa). Mature BMAds express late adipogenic genes (AdipoQ, Glut4, Ap2, LPL, PLIN1, ZFP423) [27]. In previous studies, the proportion of PPAR-γ positive cells in the bone marrow of AA murine was significantly increased, as demonstrated by immunohistochemistry. The expression was predominantly observed in the nucleus, and these positive cells were mainly localized around adipocytes. The expression of PPAR-γ in the bone marrow of AA murine was significantly upregulated according to Western blot analysis, which showed a negative correlation with both bone marrow hematopoietic volume and peripheral blood morphology. By inhibiting T cell activation, the PPAR-γ antagonist GW9662 effectively ameliorated panhemopenia and bone marrow failure in AA murine [13]. Increased expression of PPAR-γ was detected in BMMSCs from patients with AA, while its antagonist suppressed BMMSCs differentiation into adipocytes. The expression level of LPL in AA patients exhibited a negative correlation with the hematopoietic function of bone marrow. The expression levels of the Ap2 gene and protein were significantly elevated in AA patients compared to normal controls [5]. In our study, we found that the expression of adipogenesis-associated factors PPAR-γ, LPL, and Ap2 was significantly elevated in AA murine and that Rapa and CsA downregulated these genes.

This work provides several novel insights into AA pathophysiology and therapy. First, it is the first study to systematically integrate lipidomic profiling with mechanistic analyses to dissect lipid metabolism dysregulation in AA murine models, identifying glycerophospholipid metabolism as a central perturbed pathway. Second, we directly compared two immunosuppressants (Rapa and CsA) with distinct molecular targets, revealing their shared yet mechanistically divergent effects on adipogenesis and lipid storage. Third, our findings bridge immunomodulatory and metabolic axes in AA, offering a holistic framework for understanding how Rapa and CsA alleviate marrow adiposity beyond their canonical immunosuppressive roles. These strengths collectively advance AA research by linking lipid metabolic reprogramming to therapeutic efficacy, a previously underexplored dimension.

Limitations

There are some limitations to our study. The sample size was relatively small for the evaluation of treatment response of AA murine. The mechanism necessitates further investigation in future research. Future work should expand lipidomic profiling and validate PPAR-γ/NFAT crosstalk in human AA stroma.

CONCLUSION

In summary, our study demonstrated that bone marrow adiposity was upregulated, accompanied by elevated expression of adipogenesis and disrupted lipid metabolism, particularly involving glycerophospholipids in the AA murine model. The lipidomics analysis revealed that Rapa and CsA downregulate the expression of specific lipids, particularly glycerophospholipids. Furthermore, this study employed lipidomics for the first time to investigate lipid metabolism in AA murine, revealing that Rapa and CsA primarily downregulate glycerophospholipid metabolism to alleviate bone marrow adiposity in AA murine.

Source of Funds:

This work was supported by the National Natural Science Foundation of China (grant no. 82270139), Key Technology Research and Development Program of Tianjin, China (18ZXDBSY00140), and Tianjin Medical University Climbing Program Talent Project.

Declaration of Interest:

All authors declare that they have no conflicts of interest.

References:

1. Young NS. Aplastic Anemia. N Engl J Med 2018;379:1643-56. (PMID: 30354958)

2. Patel BA, Giudice V, Young NS. Immunologic effects on the haematopoietic stem cell in marrow failure. Best Pract Res Clin Haematol 2021;34:101276. (PMID: 34404528)

3. Tratwal J, Labella R, Bravenboer N, et al. Reporting Guidelines, Review of Methodological Standards, and Challenges Toward Harmonization in Bone Marrow Adiposity Research. Report of the Methodologies Working Group of the International Bone Marrow Adiposity Society. Front Endocrinol (Lausanne) 2020; 11:65. (PMID: 32180758)

4. Wang H, Leng Y, Gong Y. Bone Marrow Fat and Hematopoiesis. Front Endocrinol (Lausanne) 2018;9:694. (PMID: 30546345)

5. Tripathy NK, Singh SP, Nityanand S. Enhanced adipogenicity of bone marrow mesenchymal stem cells in aplastic anemia. Stem Cells Int 2014;2014:276862. (PMID: 24876847)

6. Locasciulli A, Oneto R, Bacigalupo A, et al. Outcome of patients with acquired aplastic anemia given first line bone marrow transplantation or immunosuppressive treatment in the last decade: a report from the European Group for Blood and Marrow Transplantation (EBMT). Haematologica 2007;92:11-8. (PMID: 17229630)

7. Frickhofen N, Heimpel H, Kaltwasser JP, Schrezenmeier H, German Aplastic Anemia Study Group. Antithymocyte globulin with or without cyclosporin A: 11-year follow-up of a randomized trial comparing treatments of aplastic anemia. Blood 2003;101:1236-42. (PMID: 12393680)

8. Panwar V, Singh A, Bhatt M, et al. Multifaceted role of mTOR (mammalian target of rapamycin) signaling pathway in human health and disease. Signal Transduct Target Ther 2023;8:375. (PMID: 37779156)

9. Feng X, Lin Z, Sun W, et al. Rapamycin is highly effective in murine models of immune-mediated bone marrow failure. Haematologica 2017;102:1691-703. (PMID: 28729300)

10. Zhao H, Gao XM, Cao XX, Zhang L, Zhou DB, Li J. Revealing serum lipidomic characteristics and potential lipid biomarkers in patients with POEMS syndrome. J Cell Mol Med 2021;25:4307-15. (PMID: 33779058)

11. Gonsalves WI, Broniowska K, Jessen E, et al. Metabolomic and Lipidomic Profiling of Bone Marrow Plasma Differentiates Patients with Monoclonal Gammopathy of Undetermined Significance from Multiple Myeloma. Sci Rep 2020;10:10250. (PMID: 32581232)

12. Lim INX, Nagree MS, Xie SZ. Lipids and the cancer stemness regulatory system in acute myeloid leukemia. Essays Biochem 2022;66:333-44. (PMID: 35996953)

13. Sato K, Feng X, Chen J, et al. PPARgamma antagonist attenuates mouse immune-mediated bone marrow failure by inhibition of T cell function. Haematologica 2016;101:57-67. (PMID: 26589913)

14. Botolin S, McCabe LR. Inhibition of PPARgamma prevents type I diabetic bone marrow adiposity but not bone loss. J Cell Physiol 2006;209:967-76. (PMID: 16972249)

15. Wright HM, Clish CB, Mikami T, et al. A synthetic antagonist for the peroxisome proliferator-activated receptor gamma inhibits adipocyte differentiation. J Biol Chem 2000;275:1873-7. (PMID: 10636887)

16. Levine B, Mizushima N, Virgin HW. Autophagy in immunity and inflammation. Nature 2011;469:323-35. (PMID: 21248839)

17. Szwed A, Kim E, Jacinto E. Regulation and metabolic functions of mTORC1 and mTORC2. Physiol Rev 2021;101:1371-426. (PMID: 33599151)

18. Chang GR, Chiu YS, Wu YY, et al. Rapamycin protects against high fat diet-induced obesity in C57BL/6J mice. J Pharmacol Sci 2009;109:496-503. (PMID: 19372632)

19. Soliman GA, Acosta-Jaquez HA, Fingar DC. mTORC1 inhibition via rapamycin promotes triacylglycerol lipolysis and release of free fatty acids in 3T3-L1 adipocytes. Lipids 2010;45:1089-100. (PMID: 21042876)

20. Holowachuk EW. Nuclear factor of activated T cell (NFAT) transcription proteins regulate genes involved in adipocyte metabolism and lipolysis. Biochem Biophys Res Commun 2007;361: 427-32. (PMID: 17651692)

21. Jiang M, Wang C, Meng Q, et al. Cyclosporin A attenuates weight gain and improves glucose tolerance in diet-induced obese mice. Molecular and Cellular Endocrinology 2013;370:96-102. (PMID: 23499865)

22. Pereira MJ, Palming J, Rizell M, et al. The immunosuppressive agents rapamycin, cyclosporin A and tacrolimus increase lipolysis, inhibit lipid storage and alter expression of genes involved in lipid metabolism in human adipose tissue. Mol Cell Endocrinol 2013;365:260-9. (PMID: 23160140)

23. Vance JE. Phospholipid Synthesis and Transport in Mammalian Cells. Traffic 2014;16:1-18. (PMID: 25243850)

24. Morita SY, Ikeda Y. Regulation of membrane phospholipid biosynthesis in mammalian cells. Biochem Pharmacol 2022;206: 115296. (PMID: 36241095)

25. Calzada E, Onguka O, Claypool SM. Phosphatidylethanolamine Metabolism in Health and Disease. Int Rev Cell Mol Biol 2016; 321:29-88. (PMID: 26811286)

26. Ruan J, Yang C, Du Y, Chen M, Han B. Plasma lipidome acts as diagnostic marker and predictor for cyclosporin response in patients with aplastic anemia. Clin Exp Med 2023;23:767-76. (PMID: 35445952)

27. Raajendiran A, Tsiloulis T, Watt MJ. Adipose tissue development and the molecular regulation of lipid metabolism. Essays Biochem 2016;60:437-50. (PMID: 27980094)